

Motion-Adaptive Digital Beamforming Technique for Multichannel SAR Systems

Juan Pablo Navarro Castillo, Rolf Scheiber, Marc Jäger, and Alberto Moreira
Microwaves and Radar Institute, German Aerospace Center (DLR)
Oberpfaffenhofen, Germany
Email: Juan.NavarroCastillo@dlr.de

Abstract—This work introduces an innovative motion-adaptive algorithm for synthetic aperture radar (SAR) airborne systems implementing digital beamforming (DBF) techniques in the along-track direction. The inherent challenges posed by temporal variations in antenna phase centers, resulting from irregular across-track baselines and attitude angles, critically affect the quality of SAR image formation due to azimuth ambiguities. A novel multichannel relative motion compensation (RelMoCo) approach is proposed to efficiently correct residual phase errors arising from these temporal variations, particularly in scenarios involving aliased azimuth spectra. Additionally, the algorithm utilizes small 2D block processing to effectively accommodate relative differences between the antenna patterns of each receiver across three dimensions: squint, off-nadir, and frequency. The performance of this approach is evaluated using real airborne SAR data collected from the DBFSAR system of the German Aerospace Center (DLR). Furthermore, the potential application of this technique in spaceborne distributed SAR systems with varying across-track baselines is discussed.

Index Terms—Digital Beamforming (DBF), Motion Compensation (MoCo), Azimuth Reconstruction, Airborne Synthetic Aperture Radar (SAR), Block Processing, Antenna Patterns.

I. INTRODUCTION

Synthetic aperture radar (SAR) technology is widely known for its different applications for remote sensing. Among them is the spaceborne high-resolution wide-swath (HRWS) imagery of the Earth's surface, where the research has developed considerably in the last decades. To overcome the constraints typically associated with conventional monostatic stripmap SAR systems, HRWS SAR concepts implement digital beamforming (DBF) solutions in the along-track (azimuth) direction [1]. Due to the necessity of a low sampling frequency in azimuth, or pulse repetition frequency (PRF), to mitigate range ambiguities and manage power consumption, the Doppler spectrum of each single channel will be aliased. If a single channel is processed alone, ambiguities in the azimuth direction will appear on the focused SAR image, considerably decreasing the quality of the processing. HRWS SAR systems use multiple apertures located along the flight path that can capture radar echoes from points on the ground simultaneously. After SAR data are collected, the information from each channel is processed through a multichannel reconstruction algorithm which filters and recombines them to obtain a resampled high-resolution ambiguity-free 2D SAR signal [1]. The principle of DBF reception is illustrated in Fig. 1.

In airborne DBF SAR systems, the reconstruction algorithms cannot perform properly if interchannel motion inconsistencies are not properly taken into account [2]. Typically, these inconsistencies can be corrected with traditional motion compensation (MoCo) algorithms [3]. However, these methods assume a non-aliased Doppler spectrum, which by definition is not the case in HRWS SAR systems. To solve this, a reconstruction algorithm is proposed in [4] to account accurately for these motion components based on the data provided by the navigation system of the aircraft. This solution exploits the properties of the DBF azimuth reconstruction to redefine the multi-channel impulse response function (IRF). This allows to perform residual motion corrections in the Doppler domain, even if the Doppler spectrum is aliased. This approach might be useful in spaceborne distributed SAR systems, where orbit control limitations and collision risk requirements could lead to deviations in the baselines between the receivers [5].

Additionally, in DBF SAR systems with not perfectly equal receiving antenna patterns, the interchannel differences between the antenna diagrams can pose a challenge for the reconstruction since they vary across three different dimensions: squint, off-nadir, and frequency. Moreover, the pointing direction of the antenna may vary over time due to the continuous changes in the attitude angles of the sensor. To account for this, the work presented in [6] proposes the use of small blocks in the reconstruction and introduces the concept of time-variant relative antenna patterns in the reconstruction.

This work presents the advantages of combining the solutions investigated in [4] and [6] to overcome the challenges imposed by residual time-variant interchannel imbalances in airborne DBF SAR systems, such as irregular motion or residual 3D differences between antenna diagrams.

This paper is organized as follows: Section II introduces the interchannel differences typical in airborne DBF SAR systems. Section III presents the motion-adaptive DBF algorithm, including relative motion compensation (RelMoCo), relative antenna pattern correction (RelAPC), and azimuth reconstruction techniques. Section IV presents experimental results with real airborne multi-channel SAR data. Section V summarizes the main contributions and findings of this article.

II. TIME-VARIANT INTERCHANNEL DIFFERENCES

In a traditional semi-active DBF SAR system with one transmitter and multiple receive antennas arranged along the

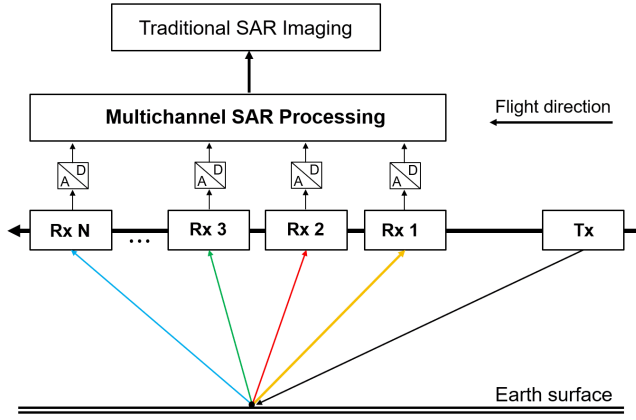


Fig. 1. Block diagram of a multi-aperture SAR system using azimuth DBF on receive. A transmitter sends a pulse (chirp) and the echoes coming from the surface are stored in multiple receivers displaced along the azimuth direction and passed to the reconstruction algorithm.

sensor track, every channel can be viewed as a bistatic SAR sensor, with the transmitter and receiver positioned apart by a specific distance in the azimuth direction, as depicted in Fig. 1. As introduced in [1], after the acquired SAR data has been compressed in the range direction, the 2D IRF of an arbitrary single bistatic channel i , where transmitter and receiver are separated in azimuth by a distance \bar{b}_{azi} , can be expressed as:

$$H_i(f_a, r; f_r) = M(f_a, r; f_r) \cdot \bar{A}_i(f_a, r; f_r) \cdot \exp\left[-j \cdot \frac{\pi}{2} \cdot \frac{f_r \cdot \bar{b}_{azi}^2}{c_0 \cdot r}\right] \cdot \exp\left[-j \cdot 2\pi \cdot f_a \cdot \frac{\bar{b}_{azi}}{2\bar{v}}\right], \quad (1)$$

where $M(f_a, r; f_r)$ is the IRF of a standard monostatic stripmap SAR system at the location of the transmitting antenna. f_r and f_a denote frequency in the range and azimuth direction, respectively. c_0 is the speed of light, r is the line-of-sight (LOS) range between the target and the sensor, and \bar{v} is the averaged speed of the sensor in the azimuth direction, which is assumed to be constant over time. $\bar{A}_i(f_a, r; f_r)$ is the effective, range-Doppler projected two-way antenna pattern of the bistatic channel i , averaged over time. As it can be observed, the bistatic IRF can be seen as a time-shifted version of the classical monostatic case with a constant phase offset and modulated by an antenna pattern [1]. The idea of traditional reconstruction algorithms is to obtain a resampled ambiguity-free version of $M(f_a, r; f_r)$ that can be then processed by a standard SAR processor to generate a focused SAR image.

A. Irregular Motion

Traditional azimuth reconstruction methods assume that the tracks are perfectly linear and that the baselines between the channels remain constant. However, this assumption does not hold for airborne platforms, where tracks are non-linear and the baselines fluctuate due to variation over time of the attitude angles, typical of airborne systems. The simplified concept of single-platform airborne motion irregularities is illustrated

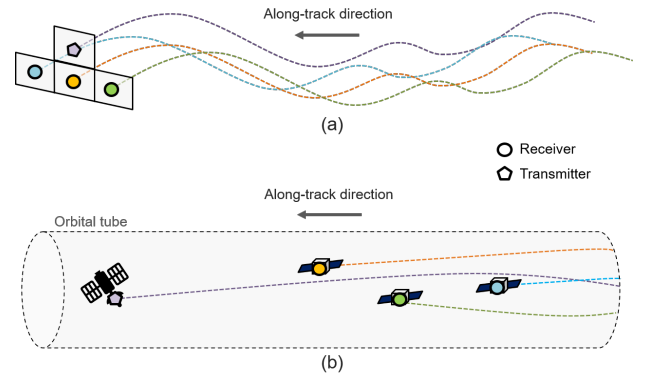


Fig. 2. Simplified illustration of the concept of across-track displacements in airborne SAR (a) and distributed SAR systems (b).

in Fig. 2(a). In this example, the DBF SAR system consists of one transmitter and three receivers mounted on the same platform. As it can be observed, the phase centers of the array present not only along-track but also across-track offsets. Additionally, these offsets will not be constant over time because of the variation of attitude angles during the flight. If these irregular motions are not addressed in a DBF airborne SAR system, it can significantly impact the performance in terms of ambiguity suppression, as demonstrated in [4]. Finally, the velocity of the sensor is not constant, which also impacts the performance of the algorithm, as can be derived from (1).

A similar challenge is being investigated in the context of spaceborne distributed SAR constellations [5]. In these HRWS SAR systems, the transmitter and receivers are mounted on different satellites and the orbital tubes are designed to be stable enough to consider the impact of across-track baselines in the azimuth reconstruction negligible. However, in a realistic scenario, this might not hold due to different constraints [5]. A simple illustration of this problem is shown in Fig. 2(b). The residual path causes phase errors that need to be properly managed during the multichannel combination process to achieve the final HRWS image.

B. Three-Dimensional Relative Antenna Patterns

In DBF SAR systems, every channel has its own receiving antenna. Ideally, the receiving radiation patterns in a DBF SAR system are intended to be nearly identical. However, in reality, there exist relative differences between the antenna patterns due to different factors, such as imperfections during the manufacturing process, the aircraft structure, coupling between the individual antenna elements, or the malfunctioning of an antenna sub-module. These relative differences between antenna diagrams can be referred to as relative antenna patterns [6]. The variation of the relative antenna patterns occurs not only in squint and off-nadir but also in the range frequency (f_r). Not accounting for the differences of the antenna pattern in these three dimensions will reduce the ambiguity suppression capabilities of the reconstruction algorithm. Finally, the variation over time of the aircraft attitude angles will modify constantly the direction of the center of the antenna beam,

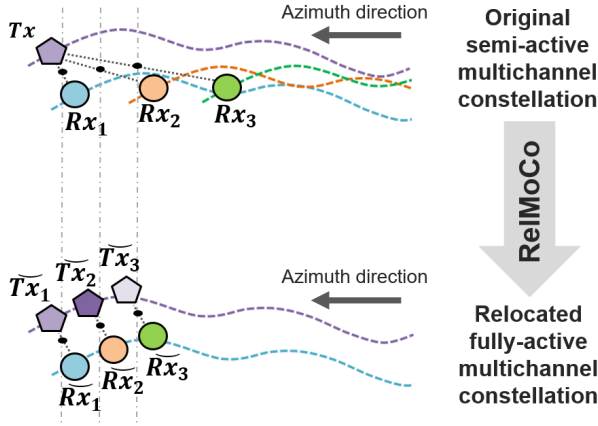


Fig. 3. Proposed transformation from a semi-active multi-static SAR formation into a fully-active multi-static SAR constellation. The black points between transmitters and receivers represent the approximated position of the phase center for each bistatic channel. In this example, Rx_1 is the reference receiver.

which will make the antenna modulation of the bistatic IRF time-variant [6]. For this reason, $\bar{A}_i(f_a, r; f_r)$ needs to be expressed as an averaged value over time in (1).

III. MOTION-ADAPTIVE AZIMUTH RECONSTRUCTION

As presented in Section I and Section II, real HRWS SAR systems are semi-active (one transmitter and multiple receivers) to avoid operation inefficiencies [7]. In [8], an innovative reconstruction algorithm including a RelMoCo approach was proposed to account for the motion irregularities in the reconstruction by relocating virtually the position of the antenna phase centers, so that the receivers follow the original path of the transmitter. In this approach, the absolute azimuth baselines b_{azi} between each receiver and the transmitter are used, as is usual in DBF SAR systems [1]. Nevertheless, in scenarios with big values of b_{azi} , the constant phase exponential component in (1) derived from a quadratic approximation is not accurate enough and leads to an increase of the azimuth-ambiguity-to-signal ratio (AASR). Moreover, the correct output geometry of the reconstructed track must be estimated carefully, since the gain and phase of all input channels are modified during this process. An incorrect estimation of this track may lead to residual azimuth position errors.

The idea of the RelMoCo approach introduced in Section III-A is to redefine the multi-channel system as an ideal fully-active multistatic constellation with multiple virtual transmitters, each of them having its own dedicated receiver. In this setup, each virtual transmitter follows the same path as the original transmitter and each receiver follows the path of the receiver of the bistatic channel that is selected to be the reference. This concept is depicted in Fig. 3, where the bistatic reference channel is the one formed by the transmitter and the receiver 1.

In this ideal constellation, the bistatic IRF of each channel can be defined as just a time-shifted version of the reference bistatic channel, where the time shift is estimated using the relative baselines between receivers instead of the azimuth baselines between the transmitter and the respective receiver. The use of relative baselines allows an easier and more accurate definition of the reconstruction filters and the output geometry since the reference bistatic channel can be kept unaltered. Then, using the change of geometry depicted in Fig. 3, the interchannel residual phase components coming from the virtual change of geometry are calculated similarly as in [8].

In the first step, as described in [4], the subsampled SAR data are processed in the time domain by a beam center RelMoCo algorithm. After this step, the fully-active bistatic IRF can be defined as:

$$G_i(f_a, r; f_r) = H_{ref}(f_a, r; f_r) \cdot \bar{A}_i(f_a, r; f_r) \cdot \bar{E}_{D_i}(f_a, r; f_r) \cdot \exp\left[-j \cdot 2\pi \cdot f_a \cdot \frac{\Delta \bar{b}_{azi}}{2v}\right], \quad (2)$$

where $\bar{E}_{D_i}(f_a, r; f_r)$ is the residual motion component calculated using the information provided by the original tracks, the relocated tracks, and a digital elevation model (DEM). $\Delta \bar{b}_{azi}$ is the relative baseline between the receiver of channel i and the reference receiver. Looking at (2), it can be derived that after reconstruction, the output signal will be a resampled version of $H_{ref}(f_a, r; f_r)$ which is the original bistatic IRF of the reference bistatic channel.

In the next section, the beam center relative motion compensation and the Doppler-dependent motion component in (2) are presented.

A. Modified Relative Motion Compensation

After the relocated tracks are calculated, the phase error derived from the motion inconsistencies can be expressed as:

$$\phi_{BC_i}(t, r; f_0) = \frac{2\pi \cdot f_0}{c_0} \cdot \Delta R_{BC_i}(t, r), \quad (3)$$

where

$$\Delta R_{BC_i}(t, r) = \Delta R_{Tx_i}(t; f_{dc}, r) + \Delta R_{Rx_i}(t; f_{dc}, r), \quad (4)$$

where $\Delta R_{Tx_i}(t; f_{dc}, r)$ and $\Delta R_{Rx_i}(t; f_{dc}, r)$ are the LOS differences between real and relocated tracks to a certain point at a range r for transmission and reception, respectively. f_0 denotes the center frequency in transmission and f_{dc} indicates the frequency Doppler centroid (FDC), which is associated with the squint direction of the antenna center beam. In this paper, it is assumed that f_{dc} is the same for each bistatic channel and constant over range. This approximation does not hold for bistatic high-squinted SAR systems with big baselines in azimuth, like in distributed SAR [9].

Supposing a subsampled range-compressed 2D dataset $s_i(t, r; f_r)$, the beam center corrected data can be defined as:

$$\hat{s}_i(t, r; f_r) = \frac{s_i(t, r + \frac{\Delta R_{BC_i}(t, r)}{2}, f_r)}{\exp[-j \cdot \phi_{BC_i}(t, r; f_0)]}, \quad (5)$$

Since the phase correction is range-dependent, an interpolation of the channel data needs to be performed before this correction happens, as expressed in (5). This reduces the residual phase error arising from the non-polychromatic definition of (3), which is just defined for the transmitted center frequency. Moreover, the interpolation in range will generate a phase modulation in azimuth that will modify the position of the real FDC in the input data due to the change of geometry.

To calculate the Doppler-dependent motion component in (2), the averaged value over time of the LOS range differences in Rx and Tx used in the beam-center RelMoCo ($\Delta\bar{R}_{BC_i}(r)$) must be subtracted from the Doppler-dependent LOS differences. Gathering all this information, this motion component can be expressed as:

$$\bar{E}_{D_i}(f_a, r; f_r) = \exp\left[-j \cdot \Delta\bar{\phi}_{D_i}(f_a, r; f_r)\right], \quad (6)$$

where

$$\Delta\bar{\phi}_{D_i}(f_a, r; f_r) = \frac{2\pi \cdot f_r}{c_0} \cdot (\Delta\bar{R}_{D_i}(f_a, r) - \Delta\bar{R}_{BC_i}(r)), \quad (7)$$

where

$$\Delta\bar{R}_{D_i}(f_a, r) = \Delta\bar{R}_{R_{x_i}}(f_a, r) + \Delta\bar{R}_{T_{x_i}}(f_a, r). \quad (8)$$

Refer to [4] for more details concerning the calculation of these relative motion components.

B. Relative Antenna Pattern Correction

Defining the bistatic IRF as in (2) will modify the input of the reference bistatic channel. As explained at the beginning of Section III, the reference bistatic channel is intended to be left unaltered to have an accurate expectation of the features of the reconstructed output. To achieve this, the nominal antenna pattern of each channel can be expressed as the product of the nominal antenna diagram of the reference channel and the interchannel antenna pattern differences between both channels.

As introduced in Section II, these differences can be referred to as relative antenna patterns and can be expressed as:

$$\Delta\bar{A}_i(f_a, r; f_r) = \frac{\bar{A}_i(f_a, r, f_r)}{\bar{A}_{ref}(f_a, r, f_r)} \quad (9)$$

where $\bar{A}_{ref}(f_a, r, f_r)$ is the projected antenna pattern of the reference channel [6]. Including (9) in (2), the bistatic IRF can be expressed as:

$$G_i(f_a, r; f_r) = \bar{W}_{ref}(f_a, r; f_r) \cdot \Delta\bar{A}_i(f_a, r; f_r) \cdot \bar{E}_{D_i}(f_a, r; f_r) \cdot \exp\left[-j \cdot 2\pi \cdot f_a \cdot \frac{\Delta\bar{b}_{azi}}{2v}\right], \quad (10)$$

where

$$\bar{W}_{ref}(f_a, r; f_r) = H_{ref}(f_a, r; f_r) \cdot \bar{A}_{ref}(f_a, r, f_r). \quad (11)$$

In addition, this modification typically aligns with the input requirements of SAR processors used to focus range-compressed SAR data. For instance, the processor of DLR's DBFSAR airborne sensor expects an antenna-modulated range-compressed dataset.

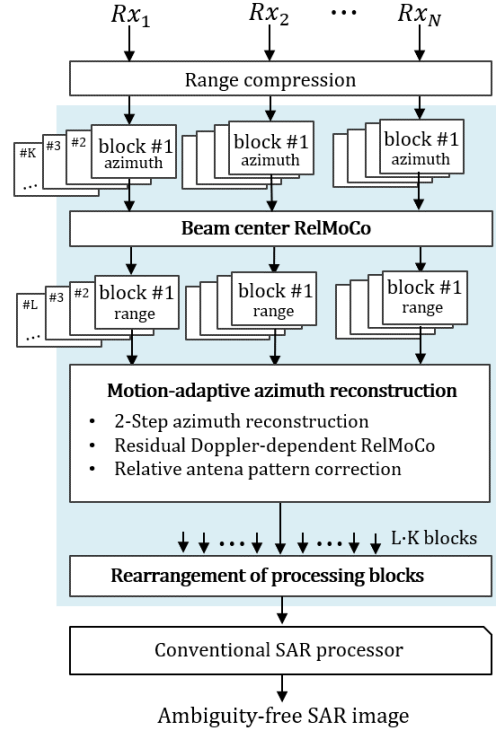


Fig. 4. The block diagram shows a simplified version of the proposed algorithm to process undersampled channels in a DBF SAR airborne system.

C. Two-Dimensional Block Processing

Finally, it is important to remark that the motion-adaptive reconstruction implements a two-step reconstruction based on the concept presented in [9] to account for a bistatic IRF which accounts for the polychromatic nature of the transmitted SAR signal. Nevertheless, in one of the steps, the reference range needs to be fixed to a certain value. As explained in [6], if the coverage of the swath is wide, the use of a single reference range for the whole image will lead to big residual errors in the reconstruction, decreasing the performance. Moreover, for SAR acquisitions with time-variant along-track velocity and attitude angles, the use of a single averaged value for the bistatic IRF is not realistic [4]. For this reason, separating the input data into small 2D blocks will increase considerably the accuracy of the reconstruction algorithm.

A block diagram showing the main components of the proposed motion-adaptive reconstruction processing chain is depicted in Fig. 4. The range block processing is implemented after the beam center RelMoCo to avoid issues at the block boundaries when doing the interpolation introduced in (5). The motion compensation of the original non-linear track and the nominal antenna pattern correction of the reference channel will take place after the reconstruction.

IV. EXPERIMENTAL RESULTS

A multichannel dataset from the DLR's DBFSAR airborne system [10] was utilized to validate the proposed reconstruction algorithm. The antenna array used in this experiment is

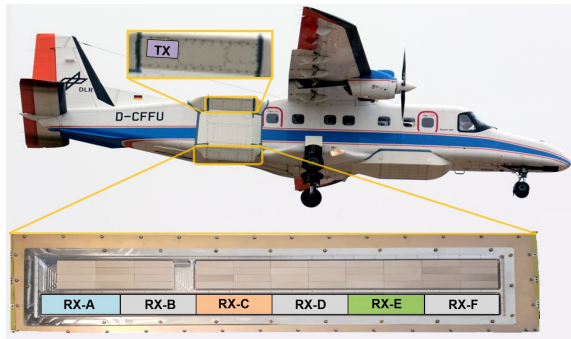


Fig. 5. DBF antenna array in the DLR DO 228-212 aircraft operating in the X-band. The colored Rx channels are the ones used in the experiments presented in this paper. The transmitter is placed above the reception array.

TABLE I
PARAMETERS DBF SAR EXPERIMENT

Parameter	Value
Average sensor height	3050 m
Mean velocity	90.11 m/s
Chirp bandwidth	400 MHz
Processed squint angle	-2.83°
Carrier frequency	9.50 GHz
Original PRF	3004.80 Hz
Number of receivers	3

shown in Fig. 5. Prior to compressing the data in range, the calibration of antenna pointing, phase center location, system delays, and relative channel phase and amplitude offsets were adjusted using the external calibration detailed in [11]. Relevant parameters for the airborne SAR flight are outlined in Table I. The 3dB azimuth bandwidth of the two-way antenna pattern was around 600 Hz. Given that the PRF was significantly greater than this bandwidth, it was necessary to preprocess the oversampled range-compressed data to simulate an undersampled scenario. This involved initially processing the data with a low-pass filter (LPF) to reduce the original azimuth bandwidth to 430 Hz while keeping the full PRF intact. Subsequently, the data were decimated by a factor of 20, removing 95% of all range lines to achieve a PRF of 150 Hz.

In this experiment, the multichannel subsampled data are processed using four different reconstruction configurations. Fig. 6 depicts a 1D plot after integrating the power of the range bins in the areas delimited by the green rectangles in Fig. 7 which depicts two different scenes from the resulting focused 2D SAR image. In scenario 1 (first column in Fig. 7), the multichannel reconstruction was performed without using any RelMoCo or RelAPC, assuming the interchannel imbalances to be negligible. Then, in scenario 2 (second column in Fig. 7), the relative motion components were accounted for by applying the RelMoCo processing steps. In scenario 3 (third column in Fig. 7), the relative antenna patterns were included in the process. The block size in scenarios 1, 2, and 3 was 64 samples in azimuth (equivalent to 38 m) and 64 in range (close to 20 m). In scenario 4 (fourth column in Fig. 7), the

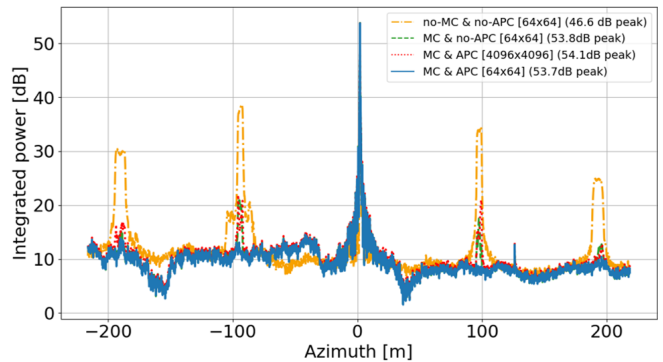


Fig. 6. Representation of the azimuth ambiguities after integrating the power of the range bins in the green squares depicted in Fig. 7. The peak power of each reconstructed point target is shown in the legend.

same setup as in scenario 3 was evaluated but the block size was increased to 4096x4096 samples.

Observing Fig. 6, Fig. 7(a) and Fig. 7(e), it becomes clear that neglecting the influence of the discussed interchannel imbalances leads to really poor performance in terms of azimuth ambiguity suppression. The reconstruction in Fig. 7(b) and Fig. 7(d) removed most of the ambiguous power from the image, but residual ambiguities are still visible on the scene. In Fig. 7(c), the reconstruction worked as expected, suppressing the azimuth ambiguities correctly and confirming the excellent performance of the proposed solution. The result in Fig. 7(d) shows the importance of using small block sizes in the reconstruction process when polychromatic time-variant interchannel imbalances are present during the radar acquisition. In Fig. 7(f), Fig. 7(g), and Fig. 7(h), the performance of the reconstruction does not show evident differences, even in the presence of areas with low clutter, like a lake. Nevertheless, a small residual azimuth ambiguity can be observed in the marked area on the bottom left side of Fig. 7(f) and Fig. 7(h). From this result, it can be interpreted that the use of small 2D block processing is especially beneficial in scenarios with strong point targets. In all cases, the azimuth resolution achieved was close to the nominal value of 23 cm.

V. CONCLUSIONS

The solution presented in this paper effectively integrates the strengths of a motion compensation algorithm with an azimuth reconstruction algorithm, resulting in improved performance for HRWS SAR systems that experience time-variant motion inconsistencies, particularly in airborne DBF SAR sensors. The innovative use of the RelMoCo algorithm facilitates a virtual adjustment of the original geometry of bistatic tracks into a more optimal configuration, simplifying the definition of the bistatic IRF. This approach exploits the capability of azimuth reconstruction algorithms for correcting interchannel imbalances, even in the presence of aliasing in the Doppler spectrum of the input data.

Moreover, employing a two-step reconstruction technique enables the accommodation of the polychromatic characteristics of SAR signals and the relative variances in two-

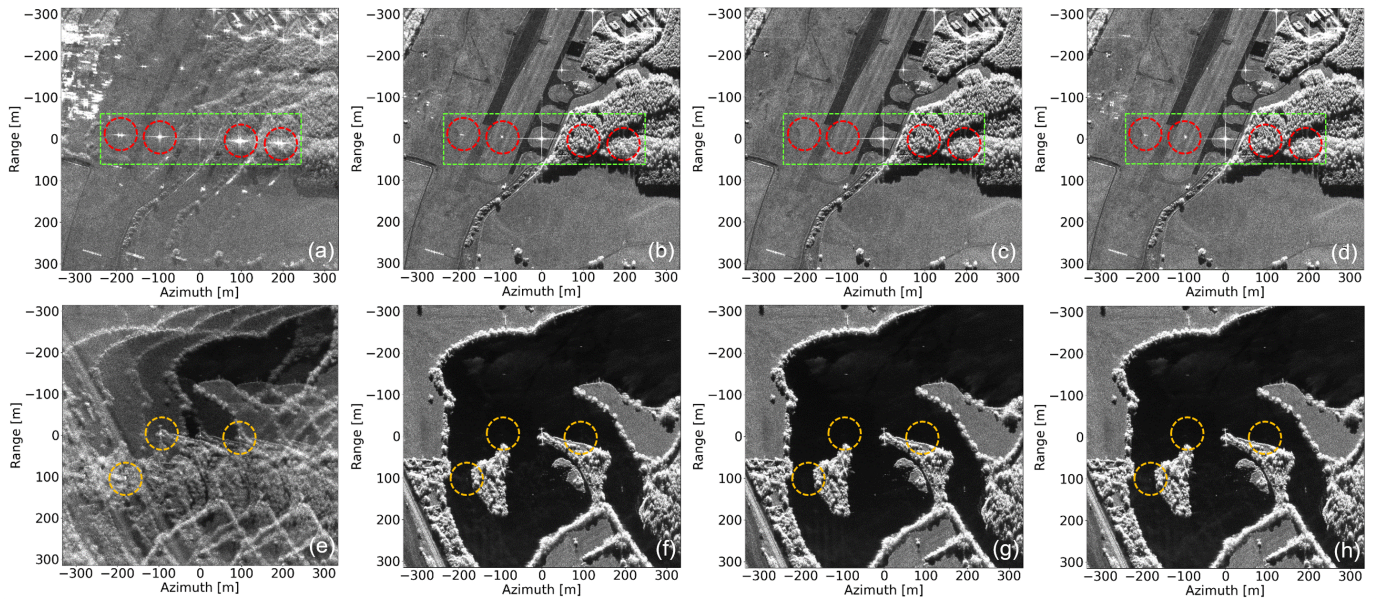


Fig. 7. Real reconstructed SAR images using different configurations for the algorithm: Reconstruction without any previous RelMoCo or RelAPC, and applying a block size of 64×64 samples (first column). Reconstruction using the RelMoCo but no RelAPC (second column), and a block size of 64×64 . Reconstruction using the RelMoCo and the RelAPC with a block size of 64×64 (third column), and 4096×4096 (fourth column). The red circles indicate the expected position of the azimuth ambiguities of the strongest point target in the scenes on the top row. The green squares indicate the area in which the power of the range bins was integrated to obtain Fig. 6. Finally, the yellow circles show the expected position of the strongest ambiguities of two natural targets located next to an area of low clutter (bottom row).

way antenna patterns across three dimensions. The results demonstrate the efficacy of the proposed algorithm and underline the significance of addressing motion inconsistencies during azimuth reconstruction. The findings also emphasize the importance of partitioning the input range-compressed data into smaller two-dimensional blocks for DBF SAR systems that face polychromatic time-variant channel imbalances, especially in the presence of strong point targets.

Additionally, while this method shows very good performance for airborne DBF SAR applications, it could also have potential advantages for spaceborne HRWS SAR systems that encounter similar issues, such as across-track baselines or time-varying attitude angles. Its applicability may be particularly advantageous for distributed SAR systems that can experience undesirable across-track offsets due to specific requirements. However, it is important to note that in this study, the assumption of a constant FDC over range and equal between channels may not hold true in bistatic scenarios where significant azimuth baselines exist between transmitter and receiver. This and other assumptions will be further investigated to assess the applicability of the proposed algorithm in spaceborne distributed SAR systems.

REFERENCES

- [1] G. Krieger, N. Gebert, and A. Moreira, "Unambiguous SAR Signal Reconstruction from Nonuniform Displaced Phase Center Sampling," *IEEE Geoscience and Remote Sensing Letters*, vol. 1, no. 4, pp. 260–264, Oct. 2004.
- [2] Z. Chen, Z. Zhang, J. Qiu, Y. Zhou, W. Wang, H. Fan, and R. Wang, "A Novel Motion Compensation Scheme for 2-D Multichannel SAR Systems with Quaternion Posture Calculation," *IEEE Transactions on Geoscience and Remote Sensing*, vol. 59, no. 11, pp. 9350–9360, Nov. 2021.
- [3] P. Prats, K. A. Camara de Macedo, A. Reigber, R. Scheiber, and J. J. Mallorqui, "Comparison of Topography- and Aperture-Dependent Motion Compensation Algorithms for Airborne SAR," *IEEE Geoscience and Remote Sensing Letters*, vol. 4, no. 3, pp. 349–353, Jul. 2007.
- [4] J. P. Navarro Castillo, R. Scheiber, M. Jäger, and A. Moreira, "Sub-Aperture Motion-Adaptive Reconstruction Techniques for Digital Beamforming Airborne SAR," *IEEE Transactions on Geoscience and Remote Sensing*, pp. 1–1, 2024.
- [5] N. Petrushevsky, A. Monti-Guarnieri, and A. Rosario Persico, "Unambiguous Imaging by a Distributed SAR System with Cross-Track Baselines," *IEEE Transactions on Geoscience and Remote Sensing*, vol. 62, pp. 1–11, 2024.
- [6] J. P. Navarro Castillo, R. Scheiber, M. Jaeger, and A. Moreira, "Inter-channel Antenna Pattern Correction for Azimuth Digital Beamforming in Airborne SAR," *IEEE Geoscience and Remote Sensing Letters*, vol. 22, pp. 1–5, 2025.
- [7] N. Sakar, M. Rodriguez-Cassola, P. Prats-Iraola, and A. Moreira, "Sampling Analysis and Processing Approach for Distributed SAR Constellations with Along-Track Baselines," *IEEE Transactions on Geoscience and Remote Sensing*, vol. 60, pp. 1–12, 2022.
- [8] J. P. Navarro Castillo, M. Jaeger, R. Scheiber, and A. Moreira, "Accurate Relative Motion Compensation for Digital Beamforming in Airborne SAR," in *EUSAR 2024; 15th European Conference on Synthetic Aperture Radar*, 2024, pp. 795–800.
- [9] N. Sakar, M. Rodriguez-Cassola, P. Prats-Iraola, and A. Moreira, "Azimuth Reconstruction Algorithm for Multistatic SAR Formations with Large Along-Track Baselines," *IEEE Transactions on Geoscience and Remote Sensing*, vol. 58, no. 3, pp. 1931–1940, Mar. 2020.
- [10] A. Reigber *et al.*, "Very-High-Resolution Airborne Synthetic Aperture Radar Imaging: Signal Processing and Applications," *Proceedings of the IEEE*, vol. 101, no. 3, pp. 759–783, Mar. 2013.
- [11] M. Jäger, R. Scheiber, and A. Reigber, "Robust, Model-Based External Calibration of Multi-Channel Airborne SAR Sensors Using Range Compressed Raw Data," *Remote Sensing*, vol. 11, no. 22, p. 2674, Nov. 2019.